Study on Dynamic Characteristics of UHVDC System under Hierarchical Infeed Mode with STATCOM

Atiq Ur REHMAN[1], *Zmarrak Wali KHAN*[2], *Bilawal REHMAN*[2], *Sheeraz IQBAL*[3], *Mehr GUL*[1]

[1]Department of Electrical Engineering, Balochistan University of Information Technology, Engineering and Management Sciences, 87300 Quetta, Pakistan
[2]State Key Laboratory of Alternate Electrical Power System with Renewable Energy Sources, North China Electric Power University, Beinong Road 2, 102206 Beijing, China
[3]Department of Electrical Engineering, University of Azad Jammu and Kashmir, Chela Campus, 13100 Muzaffarabad, Pakistan

atiq_marwat99@yahoo.com, zmarrakwali@outlook.com, eer.cbr@gmail.com, engrsheeraziqbal@gmail.com, ehrbuitms@gmail.com

DOI: 10.15598/aeee.v19i1.3937

Article history: Received Sep 03, 2020; Revised Nov 30, 2020; Accepted Jan 01, 2021; Published Mar 31, 2021.

Abstract. *This paper focuses on the investigation of the dynamic characteristics of Ultra High Voltage Direct Current (UHVDC) system Under Hierarchical Infeed Mode (UHVDC-HIM) with Static Synchronous Compensator (STATCOM). The STATCOM at the inverter side of UHVDC-HIM is developed in PSCAD/EMTDC, and their power flow equations are derived. Based on these equations, the control schemes for rectifier and inverter side of UHVDC-HIM and STATCOM are properly designed. Several dynamic characteristics indices such as Commutation Failure Immunity Index (CFII), Commutation Failure Probability Index (CFPI), fault recovery time and Temporary Overvoltage (TOV) are evaluated in detail. The impact of different sizes of STATCOM and Short Circuit Ratio (SCR) of AC sources on dynamic characteristics of UHVDC-HIM system during single-phase and three-phase faults are examined. The analysis shows that higher SCR values and greater capacity of STATCOM can make the UHVDC-HIM system less vulnerable to Commutation Failure (CF), considerably enhance the fault recovery time and effectively reduce the TOV.*

Keywords

Commutation Failure, fault recovery time, Hierarchical Infeed Mode (HIM), Line Commutated Converter, STATCOM, Temporary Overvoltage, UHVDC system.

1. Introduction

LINE Commutated Converter (LCC) based High Voltage Direct Current (HVDC) system is globally employed for asynchronous grid interconnection and transmission of bulk power from distant areas to local grids [1]. Due to greater demand for LCC-HVDC transmission, multiple converter stations have been built in close proximity. An HVDC system where multiple converters from different power transmissions are linked to the same AC bus is termed as a multi-infeed HVDC transmission system. However, the multi-infeed LCC-HVDC system faces few operational problems, such as inadequate power transfer and excessive absorption of reactive power at the inverter station, which eventually outcomes in certain stability concerns [2]. To resolve the mentioned issues, a novel UHVDC scheme referred to as Hierarchical Infeed Mode (HIM) is presented [3]. The HIM implies diverse AC voltage levels (i.e. 500 kV and 1000 kV) at the inverter

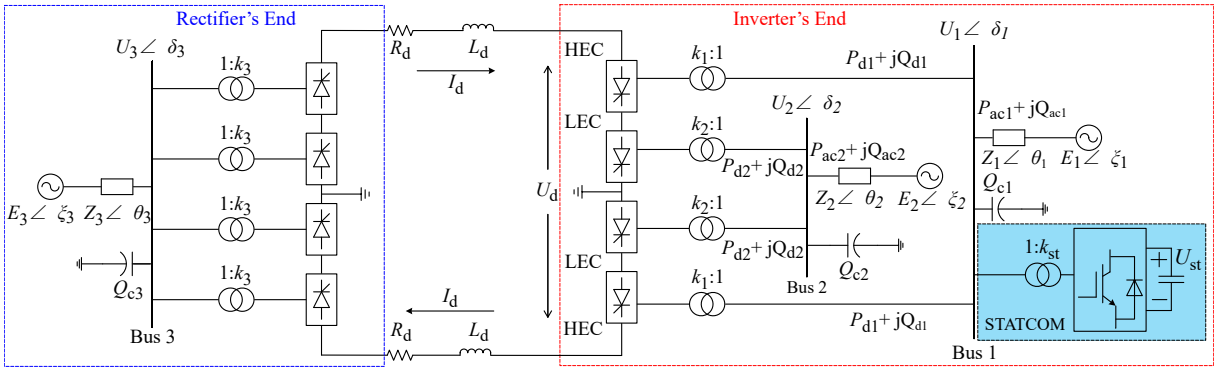

Fig. 1: Schematic diagram of UHVDC-HIM with STATCOM.

side [3]. Currently, the state grid of China employed the HIM scheme in under-construction UHVDC transmission links, such as Xilingol League to Taizhou city and Hulunbuir to Wannan [4]. The UHVDC-HIM system has many advantages, including voltage support capability, high power transmission capacity over long distances, and lesser capital cost [5]. Besides several benefits, it has some operating challenges, such as frequency deviation, Commutation Failure (CF), longer fault recovery time and high Temporary Overvoltage (TOV), specifically when the inverter station is allied to a weak AC network.

Unfortunately, not much literature exists regarding dynamic performance improvement of the UHVDC-HIM system. The power flow modeling of the UHVDC-HIM system is analyzed in [6]. Reference [4] proposed voltage stability factor for UHVDC system hierarchically embedded into grid. The stability of UHVDC-HIM is discussed in [5]. Reference [7] derived a new index as the multi-infeed short circuit ratio for UHVDC transmission hierarchically attached to AC system. Reference [8] presented a mathematical model to assess Multi-Infeed Interaction Factor (MIIF) of UHVDC-HIM. The mentioned literature has not focused on the operational challenges and dynamic characteristics assessment of UHVDC-HIM.

To overwhelmed the operating issues associated with LCC-HVDC transmission, different reactive power compensation devices like Fixed Capacitor (FC), Static Var Compensator (SVC), Synchronous Compensator (SC), and Static Synchronous Compensator (STATCOM) are used [9], [10], [11] and [12]. Reference [9] compared various compensator schemes (FC, SC, SVC, combination of SC and SVC) for LCC-HVDC transmission allied to a weak AC system. It is determined that the combination of SVC and SC gives the best performance as compared to other reactive power compensation schemes. Since STATCOM has the capability to regulate AC bus voltages and provide continuous current even under the worst system's voltage [12], it could be utilized to improve operating characteristics of LCC-HVDC transmission. Reference [12] investigates the influence of reactive power compensation devices on dynamic characteristics of LCC-HVDC transmission under lower Short Circuit Ratio (SCR) conditions. The operating issues related to LCC-HVDC transmission can also be resolved by interconnecting it with a Voltage Source Converter (VSC) based HVDC system [13]. The detail about the VSC-HVDC system can be referred to [14], [15] and [16]. As the UHVDC-HIM system is a new scheme, so it is necessary to do research that mainly focuses on dynamic characteristics improvement of the system.

Considering the capability of STATCOM to flexibly adjust AC bus voltage, this work examines the influence of STATCOM on dynamics characteristics of the UHVDC-HIM, by evaluating fault recovery time, commutation failure immunity, commutation failure probability, and TOV. The impact of different sizes of STATCOM and AC system's SCR values on operational characteristics of UHVDC-HIM system is also comprehensively elaborated. The results depict that STATCOM with larger capacity and higher SCR values can enhance dynamic characteristics of UHVDC-HIM. Moreover, it is also examined that when AC system (500 kV) is weak i.e. lower SCR values, then the impact of STATCOM on dynamic characteristics of the system is more prominent.

2. UHVDC-HIM System

2.1. Study System

To investigate the effect of STATCOM on dynamic characteristics of UHVDC-HIM as presented in Fig. 1, the system is modeled in PSCAD/EMTDC. At the rectifier's end, line commutated converters are linked to the same AC bus, whereas at the inverter's end, the Higher End Converters (HEC) are linked to bus 1 (500 kV), while Lower End Converters (LEC) are attached to bus 2 (1000 kV). Single STATCOM

(300 Mvar) and dual STATCOM (2·300 Mvar) are embedded into bus 1 to assess their influence on different operational phenomena, such as fault recovery time, commutation failure immunity, commutation failure probability and TOV of UHVDC-HIM system.

In Fig. 1, $U_1\angle\delta_1$, $U_2\angle\delta_2$ and $U_3\angle\delta_3$ are line to line voltages and their respective angles; $E_1\angle\xi_1$, $E_2\angle\xi_2$ and $E_3\angle\xi_3$ are electromotive forces and their respective angles; $Z_1\angle\theta_1$, $E_2\angle\theta_2$ and $E_3\angle\theta_3$ are equivalent impedances and their respective angels; k_1, k_2, k_3 and k_{st} are turn ratio of transformer; P_{d1}, P_{d2} and Q_{d1}, Q_{d2} are active and reactive powers of converter; P_{ac1}, P_{ac2} and Q_{ac1}, Q_{ac2} are active and reactive powers of AC sources; Q_{c1}, Q_{c2}, Q_{c3} indicates capacity of reactive power of AC filters and shunt capacitors; U_d and I_d represents DC voltage and current; L_{d2}, R_{d2} depicts inductance and resistance of DC link.

3. Mathematical Modelling

3.1. Modelling of UHVDC-HIM System

Considering the schematic diagram depicted in Fig. 1, the following power equations are derived. The DC voltage of UHVDC-HIM can be computed as Eq. (1).

$$U_{di} = 2 \cdot \left(\frac{3\sqrt{2}U_i}{\pi k_i} \cos\gamma_i - \frac{3}{\pi} X_i I_{di} \right). \tag{1}$$

The DC current can be evaluated as Eq. (2).

$$I_{di} = \frac{U_i \left[\cos\gamma_i - \cos\left(\gamma_i + \mu_i\right)\right]}{\sqrt{2}k_i X_i}, \tag{2}$$

where $i = 1$ and 2 for bus 1 and bus 2, respectively. X_i indicates leakage reactance of transformer, γ_i and μ_i are converter extinction angles and commutation overlap angles, respectively. The commutation overlap angle is given in Eq. (3).

$$\mu_i = \arccos\left(\cos\gamma_i - \frac{2X_i I_{di}}{\sqrt{2}U_{di}} \right) - \gamma_i. \tag{3}$$

The analytical expression for DC transmitted power of UHVDC-HIM is established as in Eq. (4).

$$P_{di} = U_{di} I_{di}. \tag{4}$$

The reactive power absorption by HEC and LEC can be obtained by using Eq. (5).

$$Q_{di} = P_{di} \tan\psi_i, \tag{5}$$

where:

$$\cos\psi_i = -\frac{\cos\gamma_i + \cos\left(\gamma_i + \mu_i\right)}{2}. \tag{6}$$

The expressions for real and reactive power of AC system are developed as in Eq. (7) and Eq. (8), respectively.

$$P_{aci} = \frac{\left[U_i^2 \cos\theta_i - E_i U_i \cos\left(\delta_i + \theta_i\right)\right]}{|Z_i|}. \tag{7}$$

$$Q_{aci} = \frac{\left[U_i^2 \sin\theta_i - E_i U_i \sin\left(\delta_i + \theta_i\right)\right]}{|Z_i|}. \tag{8}$$

The reactive power supplied by combined AC filters and shunt capacitors is calculated as in Eq. (9).

$$Q_{ci} = B_{ci} U_i^2, \tag{9}$$

where B_{ci} indicates the equivalent susceptance of AC filters and shunt capacitors. The real power of converters (HEC and LEC) and AC systems are related as in Eq. (10).

$$2P_{di} - P_{aci} = 0. \tag{10}$$

The relationship between reactive power of converters (HEC and LEC), AC systems and filters are given in Eq. (11).

$$2Q_{di} - Q_{aci} + Q_{ci} = 0. \tag{11}$$

When STATCOM is attached to bus 1, then Eq. (11) is modified as Eq. (12).

$$2Q_{di} - Q_{aci} + Q_{ci} + Q_s = 0, \tag{12}$$

where Q_s is reactive power supplied into UHVDC-HIM by STATCOM during transient state.

3.2. Modelling of STATCOM

The simplified single line diagram of STATCOM attached to 500 kV bus is presented in Fig. 2, in which I_1 represents three-phase AC current, U_s is three-phase AC voltage, U_c is the voltage across capacitor, R, L indicate equivalent resistances and inductances of transformer linking STATCOM to 500 kV bus, R_1 and L_1 represent equivalent resistances and inductances of converter transformer.

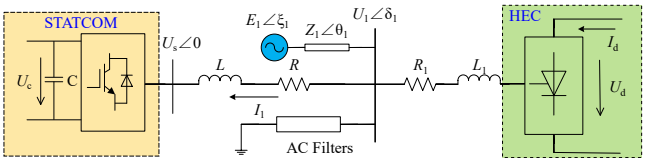

Fig. 2: Single line diagram of STATCOM linked to 500 kV bus at inverter's end.

The three-phase current (I_1) inserted to STATCOM is depicted in Eq. (13).

$$L\frac{d}{dt}\begin{bmatrix} I_{1a} \\ I_{1b} \\ I_{1c} \end{bmatrix} = \begin{bmatrix} U_{1a} \\ U_{1b} \\ U_{1c} \end{bmatrix} - \begin{bmatrix} U_{sa} \\ U_{sb} \\ U_{sc} \end{bmatrix} - R\begin{bmatrix} I_{1a} \\ I_{1b} \\ I_{1c} \end{bmatrix}. \tag{13}$$

The three-phase AC voltages of bus 1 and STATCOM are related in Eq. (14).

$$U_{sabc} = \frac{mU_c}{2} \begin{pmatrix} \sin(\omega t + \delta_1) \\ \sin(\omega t + \delta_1 - 120°) \\ \sin(\omega t + \delta_1 + 120°) \end{pmatrix}, \quad (14)$$

where δ_1 is the angle that U_s lags to U_1 and m is the modulation index. The Park's transformation matrix in Eq. (15) is utilized in order to transfer three-phase current and voltage variables into dq frame:

$$\mathbf{T}_m = \frac{2}{3} \begin{bmatrix} \cos(\omega t) & \cos(\omega t - 120°) & \cos(\omega t + 120°) \\ \sin(\omega t) & \sin(\omega t - 120°) & \sin(\omega t + 120°) \\ \frac{1}{2} & \frac{1}{2} & \frac{1}{2} \end{bmatrix}. \quad (15)$$

Applying Eq. (15) to Eq. (13), the matrix deduced as Eq. (16).

$$\begin{cases} \frac{d}{dt} I_{1d} = \frac{U_{1d} - U_{sd}}{L} - \frac{R}{L} I_{1d} + \omega I_{1q} \\ \frac{d}{dt} I_{1q} = \frac{U_{1q} - U_{sq}}{L} - \frac{R}{L} I_{1q} - \omega I_{1d} \end{cases}, \quad (16)$$

where:

$$\begin{bmatrix} U_{sd} \\ U_{sq} \end{bmatrix} = \frac{mU_c}{2} \begin{bmatrix} \sin\delta_1 \\ \cos\delta_1 \end{bmatrix}, \quad (17)$$

$$m = \frac{2\sqrt{U_{sd}^2 + U_{sq}^2}}{U_c}, \quad (18)$$

$$\delta_1 = \arctan\frac{U_{sd}}{U_{sq}}. \quad (19)$$

From Eq. (16), the following expression can be obtained.

$$\begin{cases} U_{sd} = U_{1d} - RI_{1d} - L\frac{d}{dt} I_{1d} + \omega L I_{1q} \\ U_{sq} = U_{1q} - RI_{1q} - L\frac{d}{dt} I_{1q} - \omega L I_{1d} \end{cases}. \quad (20)$$

The control strategy of UHVDC-HIM with STATCOM based on their mathematical modeling is designed and dynamic characteristics of the developed model are analyzed under various fault conditions.

4. Control Scheme of Study System

4.1. Control Scheme of UHVDC-HIM System

The control scheme of UHVDC-HIM system is given in Fig. 3. The rectifier's end is equipped with constant current control. At the inverter's end, based on Eq. (1), Eq. (2), Eq. (3) and Eq. (4), constant extinction angle control and constant current control are adopted as primary and secondary control mechanisms. The main purpose of using constant current control at the inverter's end is to maintain power flow in the DC transmission link during various disturbances at the rectifier's end. Moreover, Voltage Dependent Current Order Limiter (VDCOL) is employed at the inverter's end in order to limit DC current under the worst DC voltage.

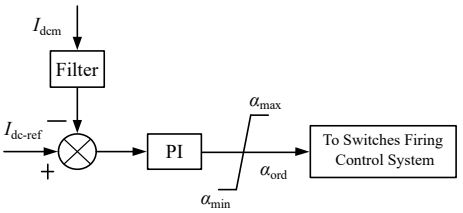

(a) Constant current control at rectifier's end.

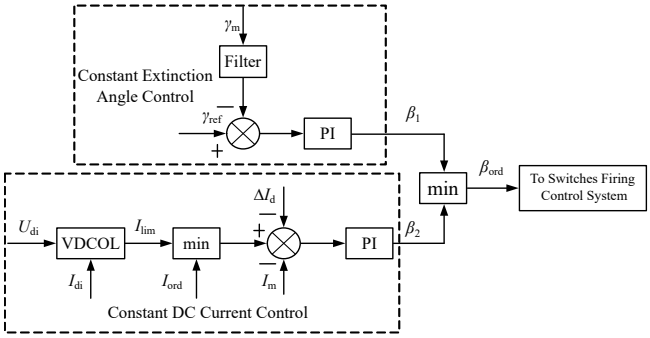

(b) Constant extinction angle and constant current control at inverter's end.

Fig. 3: Control scheme of UHVDC-HIM.

4.2. Control Scheme of STATCOM

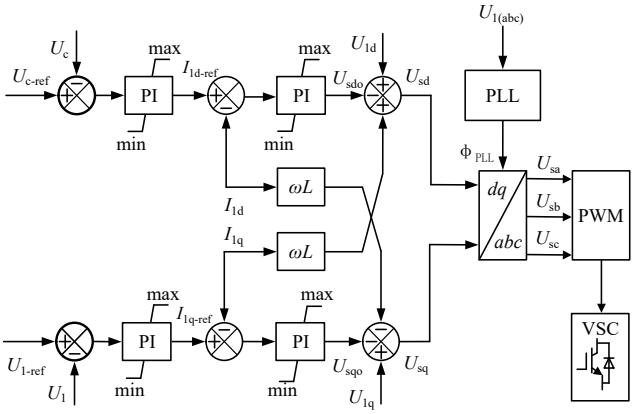

Fig. 4: Complete control scheme of STATCOM.

The overall control approach of STATCOM [17] relying on Eq. (13), Eq. (14), Eq. (15), Eq. (16), Eq. (17), Eq. (18), Eq. (19) and Eq. (20) is illustrated in Fig. 4.

It comprises of outer loop and inner loop controllers. The outer loop controllers regulate DC and AC voltages and generate d-axis and q-axis reference current (I_{1d-ref} and I_{1q-ref}). The inner loop controllers are used to adjust d-axis and q-axis currents to set with reference currents. The voltage orders (U_{sd} and U_{sq}) are produced by combining output voltages (U_{sdo} and U_{sqo}) of inner loop PI controllers, measured voltages (U_{1d} and U_{1q}) and decoupling terms (ωLI_{1q} and ωLI_{1d}). These voltage orders in *dq* frame are transformed into *abc* frame employing inverse Park's transformation, which are then utilized to produce switching signals for converters.

5. System Parameters

The real world UHVDC (±800 kV) transmission system with a rated power capacity of 10,000 MW is considered in this paper. The DC current of the system is fixed at 6.25 kA. The system AC source frequency is 50 Hz. The inverter extinction angle is set at 17°. The SCR values of 500 kV and 1000 kV AC sources at the inverter side are changed from 3 to 8. The study system for different SCR values is modified by using power flow Eq. (1), Eq. (2), Eq. (3), Eq. (4), Eq. (5), Eq. (6), Eq. (7), Eq. (8), Eq. (9), Eq. (10) and Eq. (11) of UHDC-HIM. The single STATCOM and dual STATCOM are embedded into bus 1 (500 kV) in order to assess their impact on dynamic characteristics of the UHVDC-HIM system. All other parameters of UHVDC-HIM and STATCOM are given in Tab. 1 and Tab. 2, respectively.

Tab. 1: Parameters specification of UHVDC-HIM.

Parameters	Rectifier's End	Inverter's End
AC System's Voltage	530 kV	$E_1 = 525$ kV $E_2 = 1050$ kV
AC Source Impedance Angle	$\theta_r = 84°$	$\theta_1 = 85°$ $\theta_2 = 75°$
Transformer Maximum Capacity	1527.9 MVA	1466.1 MVA
Transformer's Turn Ratio	530/172.8 kV	525/165.8 1050/165.8
Transformer's leakage Reactance	0.20 p.u.	0.20 p.u.

Tab. 2: Parameters Specification of STATCOM.

System Parameters	Value
Maximum Capacity	300 Mvar
Transformer's Turn Ratio	525/13.8
Transformer's Leakage Reactance	0.18 p.u.
Capacitance	5000.0 μF
PI Controller (DC Voltage)	$k_p = 10$, $k_i = 0.01$
PI Controller (AC Voltage)	$k_p = 10$, $k_i = 0.01$
Inner I_{1d} Controller	$k_p = 15$, $k_i = 0.001$
Inner I_{1q} Controller	$k_p = 15$, $k_i = 0.001$

6. Simulation Results

6.1. Evaluation of Commutation Failure Immunity of UHVDC-HIM System with and without STATCOM

CF is the worst dynamic event during inverter operation. It arises when converters' off-going valves endure conducting without shifting currents to ongoing valves [13]. It is obvious from Eq. (1), Eq. (2) and Eq. (3) that when AC bus voltage drops at the inverter's end of UHVDC-HIM, it will drop DC voltage and conversely increase current. The extinction angle γ_i of converters will decrease as a result of increase in commutation angle μ_i and the net effect is the occurrence of CF in the inverter station. It results in interruption of power flow to AC system. In order to mitigate CF, there is a need for dynamic reactive power compensators that can quickly bring the AC bus voltage to nominal value after clearance of fault. For this purpose, STATCOM is used to regulate AC bus voltage by supplying surplus reactive power to converter stations under various transient conditions.

Commutation Failure Immunity Index (CFII) is utilized to assess the immunity of line commutated converters to CF. CFII_i is the ratio of critical fault MVA to DC transmitted power (P_{di}) of UHVDC-HIM [18], as established in Eq. (21).

$$CFII_i(\%) = \frac{\text{Worst Critical Fault MVA}}{P_{di}} \cdot 100 = \\ = \frac{U_i^2}{\omega L_{min} P_{di}} \cdot 100. \tag{21}$$

where $i = 1, 2$ for 500 kV bus and 1000 kV bus respectively, U_i^2 indicates AC system voltage at inverter's end and L_{min} is lower inductance that does not cause CF. It is obvious from Eq. (21) that greater the fault MVA, higher will be the CFII_i value and less vulnerable is the LCC to CF. CFII_i considers HVDC controls and AC system strength and their effect on commutation process. To evaluate CFII_i, multiple run technique is developed in PSCAD/EMTDC.

The three-phase inductance fault with increasing severity is employed at the inverter's end, while continuously varying fault points on the wave. Repeated simulations are conducted for different points on wave and minimum inductance value with worst fault conditions at which CF does not occur is then utilized to evaluate CFII_i. The three-phase inductance fault is selected as it is the most severe fault as compared to resistive and capacitive that can cause CF in UHVDC-HIM.

Two cases are considered for assessing commutation failure immunity of UHVDC-HIM. When CFII_1

($CFII_2$) is calculated, three-phase inductance fault is applied into bus 1 (bus 2). In both cases, STATCOM is linked to bus 1. The feature of the two cases are:

Case 1: $CFII_1$ and $CFII_2$ values are evaluated relying on the situation that SCR_2 is set at 3 and SCR_1 value is increased from 3 to 8.

Case 2: $CFII_1$ and $CFII_2$ are assessed relying on the situation that SCR_1 is set at 3 and SCR_2 is increased from 3 to 8.

The analytical results for mentioned cases are shown in Fig. 5 and their corresponding values are given in Appendix (Tab. 4 and Tab. 5). It is clear from Fig. 5(a), that $CFII_1$ value without STATCOM is 16.97 %, with single STATCOM is 18 % and with dual STATCOM is 20.74 %. This shows that STATCOM can help UHVDC-HIM in mitigating CF. Moreover, it is also examined that for increasing SCR_1 value from 3 to 8, the $CFII_1$ value without STATCOM ranges in between 17.56 % and 61.48 %, $CFII_1$ value with single STATCOM varies from 18 % to 63.76 %, and $CFII_1$ with dual STATCOM lies in between 20.74 % and 68.85 %. This depicts that higher SCR values can enhance $CFII_1$ value.

The $CFII_2$ value with and without STATCOM is 16.95 %, as shown in Fig. 5(b). This clearly indicates that STATCOM has no influence on $CFII_2$, as there is no interconnection between two AC sources. Similarly, it can be seen from Fig. 5(c) that increasing SCR_2 value has no impact on $CFII_2$. Fig. 5(d) indicates that increasing SCR_2 value results in improving $CFII_2$ value in range of 16.95 % to 58.48 %. In this case, STATCOM has no effect on $CFII_2$ since STATCOM is connected to bus 1.

6.2. Evaluation of Commutation Failure Probability of UHVDC-HIM with and without STATCOM

To further elaborate commutation failure phenomena of UHVDC-HIM, the Commutation Failure Probability Index (CFPI) is calculated utilizing statistical program data obtained from multiple run technique of PSCAD/EMTDC simulations. CFPI is referred to as the ratio of summation of fault points resulting in CF to the total number of various fault points undertaken in a cycle [18]. The CFPI of HEC and LEC is denoted as $CFPI_1$ and $CFPI_2$, respectively. The SCR value of both AC sources is fixed at 3. As the voltage level of both buses is different, fault MVA is considered in per- unit in order to have the same fault conditions for both buses at the inverter's end. The per-unit fault level is the ratio of fault MVA to the DC transmitted power of UHVDC-HIM. The per-unit fault level for $CFPI_1$ ranges from 16 % to 25 %, and for $CFPI_2$, it lies in between 16 % and 25 %.

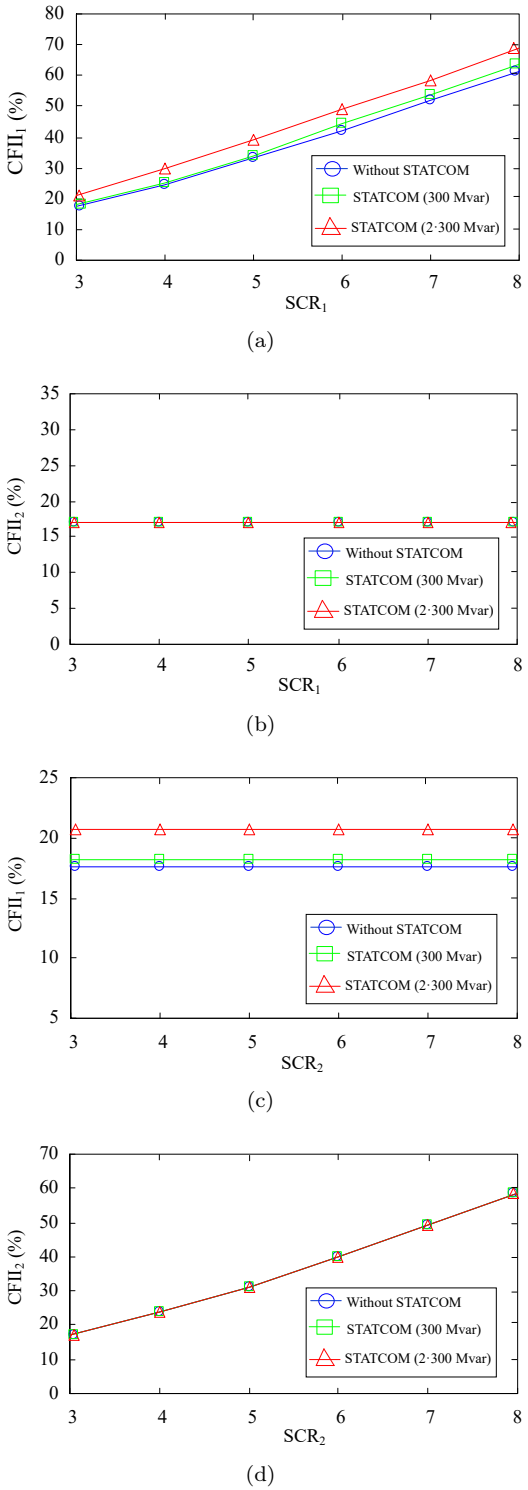

Fig. 5: $CFII_1$ and $CFII_2$ values under three-phase fault (a) and (b) **Case 1:** $SCR_2 = 3$, SCR_1 varies in range of 3 to 8. (c) and (d) **Case 2:** $SCR_1 = 3$, SCR_2 varies in range of 3 to 8.

When $CFPI_1$ ($CFPI_2$) is calculated, a three-phase inductance fault is applied into bus 1 (bus 2). For cal-

culation of $CFPI_1$ and $CFPI_2$, a total of 100 equally distributed fault points are considered in an AC cycle of 20 ms duration. The results for $CFPI_1$ and $CFPI_2$ with and without STATCOM during three-phase inductance fault with different fault levels are illustrated in Fig. 6 and Fig. 7, respectively. It is obvious from Fig. 6 that $CFPI_1$ without STATCOM is 0 for fault level less than 16.97 %. The chances of CF vary for fault level in between 16.97 and 19 %. At a higher fault level greater than 19 %, the probability of CF is 100 %. When a single STATCOM is connected to bus1, the $CFPI_1$ results are improved. The $CFPI_1$ with a single STATCOM is 0 for fault level less than 18 %, and it varies for fault level between 18 % and 19.5 %. At fault level above 19.5 %, the $CFPI_1$ with single STATCOM is 100 %. When two STATCOMs with an overall capacity of 600 Mvar are attached to bus 1, the $CFPI_1$ is reduced and there is no chance of CF up to fault level of 19.5 %. The $CFPI_1$ with dual STATCOM varies for fault level in between 19.5 % and 23 %. At fault level greater than 23 %, the $CFPI_1$ with dual STATCOM is 100 %.

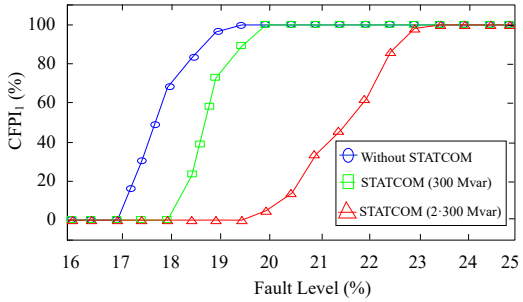

Fig. 6: $CFPI_1$ with and without STATCOM under three-phase fault.

Figure 7 indicates that $CFPI_2$ with and without STATCOM is 0 for fault level less than 16.95 %. The chances of CF increase with severe fault level and it reaches 100 % at 18.3 % fault level. It is observed that at higher fault level, the chances of CF in HEC are higher as compared to LEC. Moreover, it is also obvious from Fig. 7 that STATCOM has no contribution in improving $CFPI_2$. The results of Fig. 6 are consistent with the results presented in Fig. 5(b) and Fig. 5(d).

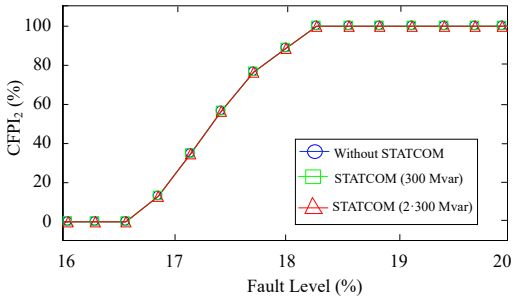

Fig. 7: $CFPI_2$ with and without STATCOM under three-phase fault.

Thus it is concluded from the above results that chances of CF in HEC and LEC are higher at sever fault conditions. At lower fault level, the $CFPI_1$ can be reduced by 1.03 % with single STATCOM and 2.53 % with dual STATCOM. At higher fault level, the $CFPI_1$ can be improved by 0.5 % with single STATCOM and 4 % with dual STATCOM.

6.3. Evaluation of Fault Recovery Performance of UHVDC-HIM with and without STATCOM

In this paper, DC power recovery time is utilized as fundamental metric to assess the fault recovery time of UHVDC-HIM quantitatively. Fault recovery time is termed as the time taken by DC power to reinstate to 90 % of pre-fault value after clearance of fault [19]. To investigate the fault recovery time of UHVDC-HIM with and without STATCOM, single-phase and three-phase faults are applied into bus 1.

1) Single-Phase Fault at Bus 1

Initially, SCR_1 and SCR_2 of the developed system given in Fig. 1 are fixed at 3. A single-phase to ground fault with 0.15 H inductor is applied at 2.0 s and lasts for five cycles (0.1 s) duration. Here, 0.15 H is the critical inductance value at which the studied system cannot experience CF under single-phase fault. The fault recovery time with and without STATCOM is shown in Fig. 8. It is examined that fault recovery time without STATCOM is 194 ms, which is very high. The fault recovery time with single and dual STATCOM is 169 ms and 52 ms, respectively. This depicts that STATCOM can reduce the faulty recovery time of UHVDC-HIM, by supplying surplus reactive power into the system at the instant of fault.

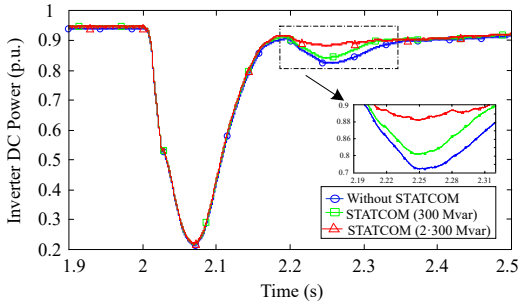

Fig. 8: DC power of bus 1 under single-phase fault, $SCR_1 = SCR_2 = 3$.

To evaluate the influence of AC system strength on fault recovery time, SCR_2 is kept constant at 3 and SCR_1 value is changed from 3 to 8. The results for fault recovery time of UHVDC-HIM with and without

STATCOM are shown in Fig. 9 and their corresponding values are summarized in Appendix (Tab. 6).

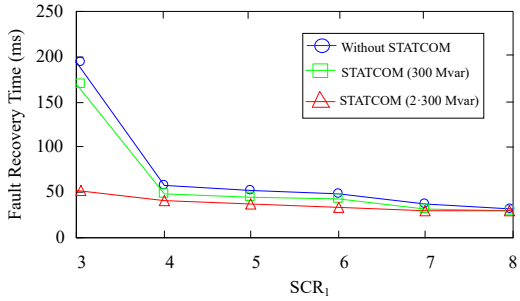

Fig. 9: Fault recovery time under single-phase fault at bus 1 for $SCR_2 = 3$ and SCR_1 varies from 3 to 8.

The fault recovery time without STATCOM decreases from 194 ms to 32 ms, when SCR_1 value increases from 3 to 8. With single STATCOM, the fault recovery time reduces from 169 ms to 29 ms. And with dual STATCOM, the fault recovery time decreases from 52 ms to 29 ms when the SCR_1 value varies from 3 to 8. This indicates that the system with low SCR_1 values has larger fault recovery times and vice versa. Moreover, it is also observed that the impact of STATCOM is more prominent for the system having low SCR_1 values. As SCR_1 value increases from 3 to 8, the impact of STATCOM on improving fault recovery time decreases.

2) Three-Phase Fault at Bus 1

Initially, SCR_1 and SCR_2 of the developed system given in Fig. 1 are fixed at 3. The five cycles (0.1 s duration) three-phase to ground fault with 0.25 H inductor is applied at 2.0 s. Here, 0.25 H is the critical inductance value at which the studied system cannot experience commutation failure under a three-phase fault. The fault recovery time with and without STATCOM is presented in Fig. 10. It is observed from Fig. 10 that fault recovery time without STATCOM is 270 ms, with single STATCOM is 240 ms and with dual STATCOM is 230 ms. This indicates that the addition of STATCOM into the UHVDC-HIM system can help in improving the fault recovery time.

To analyze the effect of system strength on fault recovery time under three-phase fault, the SCR_1 value is varied from 3 to 8 and SCR_2 is fixed at 3. The results are illustrated in Fig. 11 and their corresponding values are given in Appendix (Tab. 7). The fault recovery time without STATCOM decreases from 270 ms to 34 ms when SCR_1 value increases from 3 to 8. With single STATCOM, the fault recovery time reduces from 240 ms to 30 ms. And with dual STATCOM, the fault recovery time decreases from 230 ms to 30 ms when SCR_1 value varies from 3 to 8. It is examined that fault recovery time under three-phase fault is higher as compared to fault recovery time during single-phase fault.

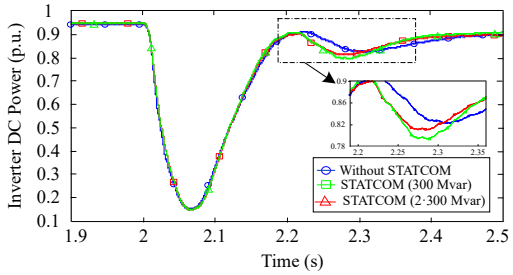

Fig. 10: DC power of bus 1 under three-phase fault, $SCR_1 = SCR_2 = 3$.

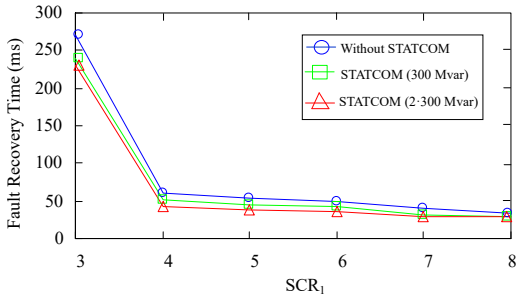

Fig. 11: Fault recovery time under three-phase fault at bus 1 for $SCR_2 = 3$ and SCR_1 varies from 3 to 8.

6.4. Investigation of TOV under Converter Blocks of LCC-UHVDC-HIM with STATCOM

LCC–HVDC station absorbs reactive power in range of 0.5 to 0.6 p.u. of rated transmitted DC power [16], which is usually supplied by filters and fixed capacitors connected to AC bus. The reactive power consumption is negligible when converters are blocked. The excessive reactive power supplied by filters and shunt capacitors results in temporary overvoltage. The case is most severe at the inverter side when AC system is weak. TOV greatly depends on AC system's impedance, angle and reactive power compensating devices connected to AC bus.

In this paper, TOV of bus 1 (TOV_1) is examined while blocking both HEC of the system.

Initially, SCR_1 and SCR_2 of the developed system are fixed at 3. It is evaluated that TOV_1 without STATCOM is 1.24 p.u., with single STATCOM is 1.21 p.u. and with dual STATCOM is 1.17 p.u. This indicates that STATCOM can support UHVDC-HIM in reducing TOV_1.

In order to assess the effect of system strength on TOV_1, the SCR_1 value is increased from 3 to 8. The TOV_1 with and without STATCOM, evaluated for different SCR_1 values ($SCR_2 = 3$), are shown in Fig. 12 and their associated values are given in Tab. 3. The TOV_1 without STACOM reduces from 1.24 to 1.08 p.u. when SCR_1 value changes from 3 to 8. With single STATCOM, the TOV_1 decreases from 1.21 to 1.06 p.u. and with dual STATCOM, the TOV_1 reduces from 1.17 to 1.03 p.u. The improvement in TOV_1 with STATCOM is because of the fact that STATCOM absorbs surplus reactive power in case when both HEC are blocked. It is thus concluded that higher SCR_1 values and greater STATCOM capacity can result in a lower value of TOV_1.

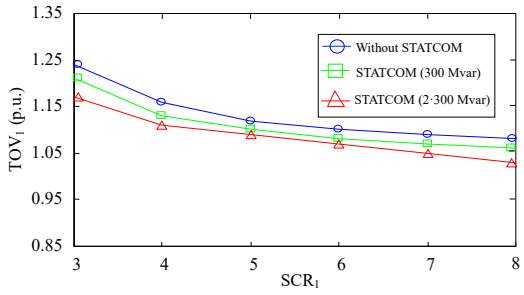

Fig. 12: TOV of bus 1 (TOV_1) with and without STATCOM for $SCR_2 = 3$ and SCR_1 value varies from 3 to 8.

Tab. 3: TOV of bus 1 with and without STATCOM for $SCR_2 = 3$, SCR_1 varies from 3 to 8.

SCR_1	Temporary Overvoltage of Bus 1 (TOV_1 p.u.)		
	Without STATCOM	STATCOM (300 Mvar)	STATCOM (2·300 Mvar)
3	1.24	1.21	1.17
4	1.16	1.13	1.11
5	1.12	1.10	1.09
6	1.10	1.08	1.07
7	1.09	1.07	1.05
8	1.08	1.06	1.03

The TOV of bus 2 (TOV_2) is assessed while blocking both LEC. The results for TOV_2 with and without STATCOM for different SCR_2 values ($SCR_1 = 3$) are shown in Fig. 13. The TOV_2 with and without STATCOM varies from 1.12 to 1.04 p.u., when SCR_1 value ranges between 3 and 8. The TOV_2 is lower than TOV_1 due to the reason that source 2 has a lower impedance angle as compared to source 1. The results also indicate that the greater the SCR_2 value, the lower will be TOV_2 and vice versa. However, STATCOM connected to bus 1 has no contribution in reducing the temporary overvoltage of bus 2.

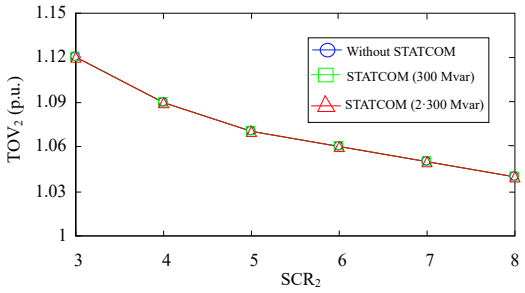

Fig. 13: TOV of bus 2 (TOV_2) with and without STATCOM for $SCR_1 = 3$ and SCR_2 value varies from 3 to 8.

7. Conclusion

In this paper, the dynamic characteristics of UHVDC transmission system under HIM with STATCOM are analyzed. Voltage source converter based STATCOM and LCC based UHVDC-HIM model is developed in PSCAD/EMTDC. The dynamic characteristics like commutation failure immunity, commutation failure probability, fault recovery time and temporary overvoltage of UHVDC-HIM are examined while considering the impact of system's strength and capacity of STATCOM. The following conclusions can be drawn from simulation results:

- STATCOM can make UHVDC-HIM less vulnerable to CF by improving $CFII_1$. When SCR_1 and SCR_2 values of AC systems are increased, the improvements in $CFII_1$ and $CFII_2$ are observed.
- The commutation failure probability index ($CFPI_1$ and $CFPI_2$) is effectively decreased with STATCOM and by using larger SCR_1 and SCR_2 values of AC sources.
- The fault recovery time under single-phase and three-phase faults is improved when single and dual STATCOM is connected at bus 1 of UHVDC-HIM.
- The temporary overvoltage of bus 1 is considerably reduced with STATCOM when both high end converters are blocked. The TOV_1 and TOV_2 can also be reduced if higher SCR_1 and SCR_2 values are considered for the AC systems.
- Moreover, it is also observed that the impact of STATCOM will be more apparent in case the AC system's SCR value is low.
- This paper can be used as a technical reference regarding dynamic characteristics analysis of UHVDC-HIM system with and without STATCOM.

Author Contributions

A.U. designed the model and analysed the data, Z.W. carried out the simulations, B.R. and S.I. contributed to the interpretation of results, M.G. wrote the paper with input from all authors.

References

[1] KWON, D.-H., Y.-J. KIM and S.-I. MOON. Modeling and Analysis of an LCC HVDC System Using DC Voltage Control to Improve Transient Response and Short-Term Power Transfer Capability. *IEEE Transactions on Power Delivery*. 2018, vol. 33, iss. 4, pp. 1922–1933. ISSN 1937-4208. DOI: 10.1109/TPWRD.2018.2805905.

[2] SHU, Y., G. CHEN, Z. YU, J. ZHANG, C. WANG and C. ZHENG. Characteristic analysis of UHVAC/DC hybrid power grids and construction of power system protection. *CSEE Journal of Power and Energy Systems*. 2017, vol. 3, iss. 4, pp. 325–333. ISSN 2096-0042. DOI: 10.17775/CSEEJPES.2017.00940.

[3] LIU, Z., X. QIN, L. ZHAO and Q. ZHAO. Study on the application of UHVDC hierarchical connection mode to multi-infeed HVDC system. *Proceedings of the Chinese Society of Electrical Engineering*. 2013, iss. 10, pp. 1–7. ISSN 0258-8013.

[4] WANG, C., L. ZHU, B. CHEN, Y. TANG and Y. DAI. Analysis on voltage stability of hybrid system with UHVDC hierarchical connection to AC grid. In: *2016 IEEE 8th International Power Electronics and Motion Control Conference (IPEMC-ECCE Asia)*. Hefei: IEEE, 2016, pp. 690–695. IEEE. ISBN 978-1-5090-1210-7. DOI: 10.1109/IPEMC.2016.7512369.

[5] TANG, Y., F. LI, Q. WANG, B. CHEN, Y.-L. JIANG and X.-J. GUO. Power stability analysis of UHVDC systems hierarchically connected to AC systems. *Electric Power Systems Research*. 2018, vol. 163, iss. 1, pp. 715–724. ISSN 0378-7796. DOI: 10.1016/j.epsr.2017.08.037.

[6] LI, S., Z. WU and J. HUANG. Power flow modelling to UHVDC line and its hierarchical connection mode. *IET Generation, Transmission & Distribution*. 2017, vol. 12, iss. 7, pp. 1554–1564. ISSN 1751-8695. DOI: 10.1049/iet-gtd.2017.0851.

[7] GUAN-HAO, Y. and Z. YAN. System Static Safety Analysis Under Multi-UHVDC Hierarchically Infeed Mode. In: *11th IET International Conference on AC and DC Power Transmission*. Birmingham: IET, 2015, pp. 1–8. ISBN 978-1-84919-982-7. DOI: 10.1049/cp.2015.0098.

[8] SUN, W., R. FU, Z. ZHOU, X. HUANG, C. WANG, K. XU, B. XIE, Z. LI and M. NI. Analysis on the operating characteristic of UHVDC hierarchical connection mode to AC system. In: *2015 5th International Conference on Electric Utility Deregulation and Restructuring and Power Technologies (DRPT)*. Changsha: IEEE, 2015, pp. 1834–1837. ISBN 978-1-4673-7106-3. DOI: 10.1109/DRPT.2015.7432543.

[9] NAYAK, O. B., A. M. GOLE, D. G. CHAPMAN and J. B. DAVIES. Dynamic performance of static and synchronous compensators at an HVDC inverter bus in a very weak AC system. *IEEE Transactions on Power Systems*. 1994, vol. 9, iss. 3, pp. 1350–1358. ISSN 1558-0679. DOI: 10.1109/59.336131.

[10] ZHUANG, Y., R. W. MENZIES, O. B. NAYAK and H. M. TURANLI. Dynamic performance of a STATCON at an HVDC inverter feeding a very weak AC system. *IEEE Transactions on Power Delivery*. 1996, vol. 11, iss. 2, pp. 958–964. ISSN 1937-4208. DOI: 10.1109/61.489357.

[11] KIM, C.-K. Dynamic coordination strategies between HVDC and STATCOM. In: *2009 Transmission & Distribution Conference & Exposition: Asia and Pacific*. Seoul: IEEE, 2009, pp. 1–9. ISBN 978-1-4244-5230-9. DOI: 10.1109/TD-ASIA.2009.5356941.

[12] ZHANG, Y. and A. M. GOLE. Comparison of the transient performance of STATCOM and Synchronous condenser at HVDC converter stations. In: *11th IET International Conference on AC and DC Power Transmission*. Birmingham: IET, 2015, pp. 1–8. ISBN 978-1-84919-982-7. DOI: 10.1049/cp.2015.0069.

[13] GUO, C., Y. ZHANG, A. M. GOLE and C. ZHAO. Analysis of Dual-Infeed HVDC With LCC–HVDC and VSC–HVDC. *IEEE Transactions on Power Delivery*. 2012, vol. 27, iss. 3, pp. 1529–1537. ISSN 1937-4208. DOI: 10.1109/TPWRD.2012.2189139.

[14] JOVCIC, D. *High voltage direct current transmission: converters, systems and DC grids*. 2nd ed. New York: John Wiley & Sons, 2019. ISBN 978-1-119-56654-0.

[15] ELGEZIRY, M. Z, M. A. ELSADD, N. I. ELKALASHY, T. A. KAWADY, A.-M. I. TAALAB and M. A. IZZULARAB. Non-pilot protection scheme for multi-terminal VSC–HVDC transmission systems. *IET Renewable Power Generation*. 2019,

vol. 13, iss. 16, pp. 3033–3042. ISSN 1752-1424. DOI: 10.1049/iet-rpg.2018.6265.

[16] ELGEZIRY, M. Z, M. A. ELSADD, N. I. ELKALASHY, T. A. KAWADY and A.-M. I. TAALAB. AC spectrum analysis for detecting DC faults on HVDC systems. In: *2017 Nineteenth International Middle East Power Systems Conference (MEPCON)*. Cairo: IEEE, 2017, pp. 708–715. ISBN 978-1-5386-0990-3. DOI: 10.1109/MEPCON.2017.8301259.

[17] SCHAUDER, C. and H. MEHTA. Vector analysis and control of advanced static VAR compensators. *IEE Proceedings C (Generation, Transmission and Distribution)*. 1993, vol. 140, iss. 4, pp. 299–306. ISSN 2053-7921. DOI: 10.1049/ip-c.1993.0044.

[18] RAHIMI, E., A. M. GOLE, J. B. DAVIES, I. T. FERNANDO and K. L. KENT. Commutation Failure Analysis in Multi-Infeed HVDC Systems. *IEEE Transactions on Power Delivery*. 2010, vol. 26, iss. 1, pp. 378–384. ISSN 1937-4208. DOI: 10.1109/TPWRD.2010.2081692.

[19] IEEE Standard 1204-1997. *IEEE Guide for Planning DC Links Terminating at AC Locations Having Low Short-Circuit Capacities*. New York: IEEE, 1997.

About Authors

Atiq Ur REHMAN was born in Khyber Pakhtunkhwa, Pakistan. He received M.Sc. degree in Electrical Engineering from University of Engineering and Technology (UET), Peshawar, Pakistan, in 2013. In 2020, he obtained Ph.D. degree in power system and it's automation from North China Electric Power University (NCEPU), Beijing, China. Currently, he is working as an Assistant Professor in Electrical Engineering Department, Balochistan University of Information Technology, Engineering and Management Sciences (BUITEMS), Quetta, Pakistan. His research interests includes HVDC and FACTS devices.

Zmarrak Wali KHAN was born in Khyber Pakhtunkhwa, Pakistan. He received M.Sc. degree in Electrical Engineering from CECOS University, Peshawar, Pakistan in 2016. He is currently pursuing Ph.D. degree in Electrical Engineering from North China Electric Power University, China. His current interest lies in the field of VSC-HVDC, MMC-HVDC and high power dc-dc converters.

Bilawal REHMAN was born in Punjab, Pakistan. He received M.Sc. degree in electrical engineering from University of Management and Technology, Lahore, Pakistan, in 2012. He has obtained Ph.D. degree in power system and automation from North China Electric Power University, Beijing, China. His research interests include HVDC operation, control and AC/DC power flow.

Sheeraz IQBAL was born in Azad Jammu and Kashmir, Pakistan. He received M.Sc. degree in electronic engineering from International Islamic University, Islamabad, Pakistan; and Ph.D. degree in Electrical Engineering from North China Electric Power University (NCEPU), Beijing China in 2014 and 2020 respectively. He is serving as Assistant Professor at department of Electrical Engineering University of Azad Jammu and Kashmir, Muzaffarabad, Pakistan. His research interests include microgrid and transactive energy.

Mehr GUL was born in Pakistan. He received M.Sc. degree in electrical engineering from MUET Jamshoro Pakistan. He completed Ph.D. degree in electrical engineering from Shanghai Jiao Tong University, Shanghai, China. He is currently an Assistant Professor in Department of Electrical Engineering, BUITEMS, Quetta, Pakistan. His area of research interest is renewable energy and HVDC networks.

Appendix A

Tab. 4: $CFII_1$ values with and without STATCOM for $SCR_2 = 3$, SCR_1 varies from 3 to 8.

SCR_1	$CFII_1$ (%)		
	Without STATCOM	STATCOM (300 Mvar)	STATCOM (2·300 Mvar)
3	16.97	18	20.74
4	24.59	25.32	29.68
5	33.10	33.75	39.12
6	41.98	44.14	49.18
7	52.16	53.79	57.38
8	61.48	63.76	68.85

Tab. 5: $CFII_2$ values with and without STATCOM for $SCR_1 = 3$, SCR_2 varies from 3 to 8.

SCR_2	$CFII_2$ (%)		
	Without STATCOM	STATCOM (300 Mvar)	STATCOM (2·300 Mvar)
3	16.95	16.95	16.95
4	24.04	24.04	24.04
5	31.33	31.33	31.33
6	40.11	40.11	40.11
7	49.08	49.08	49.08
8	58.48	58.48	58.48

Tab. 6: Fault recovery time during single-phase fault at bus 1 for $SCR_2 = 3$ and SCR_1 varies from 3 to 8.

SCR_1	Fault Recovery Time (ms)		
	Without STATCOM	STATCOM (300 Mvar)	STATCOM (2·300 Mvar)
3	194	169	52
4	57	49	41
5	52	45	38
6	48	43	34
7	38	31	30
8	32	29	29

Tab. 7: Fault recovery time during three-phase fault at bus 1 for $SCR_2 = 3$ and SCR_1 varies from 3 to 8.

SCR_1	Fault Recovery Time (ms)		
	Without STATCOM	STATCOM (300 Mvar)	STATCOM (2·300 Mvar)
3	270	240	230
4	61	51	42
5	53	45	37
6	49	42	35
7	40	32	30
8	34	30	28